Instituto de Física
Universidade de São Paulo

Micro-Raman analysis of cubic GaN layers grown by MBE on (001) GaAs substrate

Tabata, A.
Instituto de Física da Universidade de São Paulo, São Paulo, Brasil
Faculdade de Ciências de Bauru, Bauru, SP, Brasil

Lima, A.P.; Leite, J.R.
Instituto de Física da Universidade de São Paulo, São Paulo, Brasil
Faculdade de Ciências de Bauru, Bauru, SP, Brasil

Lemos, V.
Instituto de Física 'Gleb Wataghin' da Universidade Estadual de Campinas, Campinas, SP, Brasil
Faculdade de Ciências de Bauru, Bauru, SP, Brasil

Schikora, D.; Schöttker, B.; Köhler, U.; As, D.J.; Lischka, K.
FB-6 Physik, Universität Paderborn, Paderborn, Alemanha

Publicação IF - 1360/99

Semicond. Sci. Technol. **14** (1999) 318–322. Printed in the UK PII: S0268-1242(99)97926-9

Micro-Raman analysis of cubic GaN layers grown by MBE on (001) GaAs substrate

A Tabata†‡¶, A P Lima†, J R Leite†, V Lemos§, D Schikora‖, B Schöttker‖, U Köhler‖, D J As‖ and K Lischka‖

† Instituto de Física, Universidade de São Paulo, CP 66318, 05389-970, São Paulo, SP, Brazil
‡ Faculdade de Ciências de Bauru, Universidade Estadual Paulista, CP 473, 17033-360, Bauru, SP, Brazil
§ Instituto de Física 'Gleb Watagin', Universidade de Campinas, 13083-970 Campinas, SP, Brazil
‖ FB-6 Physik, Universität Paderborn, Warburger Str. 100, 33098 Paderborn, Germany

Received 29 September 1998, accepted for publication 17 December 1998

Abstract. Cubic GaN layers are grown by molecular beam epitaxy on (001) GaAs substrates. Optical micrographs of the GaN epilayers intentionally grown at Ga excess reveal the existence of surface irregularities such as bright rectangular structures, dark dots surrounded by rectangles and dark dots without rectangles. Micro-Raman spectroscopy is used to study the structural properties of these inclusions and of the epilayers in greater detail. We conclude that the observed irregularities are the result of a melting process due to the existence of a liquid Ga phase on the growing surface.

1. Introduction

Heteroepitaxial growth of zincblende-type GaN is one of the most challenging problems of current materials research. Several groups have successfully performed growth experiments by means of molecular beam epitaxy (MBE) using (001) GaAs as the substrate [1–6]. The surface reconstruction diagram of cubic GaN was determined and has been used to adjust the growth stoichiometry and to control the phase purity of the epitaxial layers. Samples grown under carefully controlled stoichiometric conditions with $c(2 \times 2)$ surface reconstruction show photoluminescence spectra which reveal the homogeneity of the cubic epilayers [6]. To determine the phase purity of the layers, various methods such as x-ray diffraction [3] and Raman spectroscopy [7–9] have been used and the crucial role of surface stoichiometry was clearly confirmed by these measurements. It was found that small deviations from ideal stoichiometry towards N-rich conditions affect the growth stability and initiate the formation of wurtzite clusters in the cubic lattice [2]. In the present paper, microcrystals and well-ordered rectangular inclusions in the GaN (001) surface, which are connected with the presence of a certain Ga excess, are investigated by means of micro-Raman spectroscopy. This method allows us to collect Raman signals from the microcrystal directly and also from parts of the epilayers which are free of any inclusions. These spectra are compared with the spectra from inclusions to allow conclusions to be drawn about the structure and the perfection of the epilayer.

¶ E-mail address: tabata@if.usp.br

2. Growth and surface morphology

The samples are grown on GaAs (001) substrates by plasma-assisted MBE using a RIBER 32 system equipped with elemental sources of Ga and As and an Oxford Applied Research CARS25 RF activated plasma source. The N_2 background pressure in the growth chamber was varied between 2×10^{-4} and 5×10^{-3} Pa. Before the cubic GaN nucleation was started, a GaAs buffer layer was grown first at 600 °C under (2×4) reconstruction to ensure As-stabilized conditions. The nucleation of cubic GaN was initiated at the same temperature using an N:Ga flux ratio of about 4. After deposition of about 10–20 monolayers, nucleation was stopped and the substrate temperature was subsequently raised to 740 °C. The growth was then continued at the higher temperature level with the N:Ga flux ratio being varied between 0.5 and 1. The growth process was monitored continuously by reflection high-energy electron diffraction (RHEED) and a RHEED image recording system. After the growth was finished, samples were etched in HCl in order to remove excess Ga from the surface.

The surface morphology of the epilayers has been studied by means of optical microscopy and atomic force microscopy (AFM). AFM measurements were performed in contact and force detection modes, using various scan widths from 100 to 4.2 μm.

Figure 1 shows a typical optical micrograph of the GaN epilayer surface taken with an optical Zeiss microscope. The resolution was 1 μm. Three kinds of irregularities are seen at the surface of a sample grown under relatively high Ga excess.

0268-1242/99/040318+05$19.50

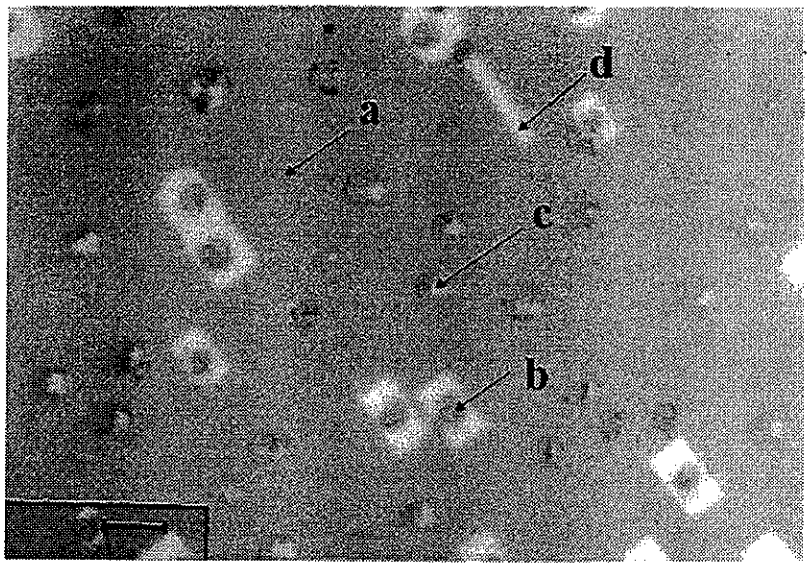

Figure 1. Typical microphotograph showing the surface morphology of our cubic GaN epilayers. The scale bar in the lower left corner corresponds to 10 μm.

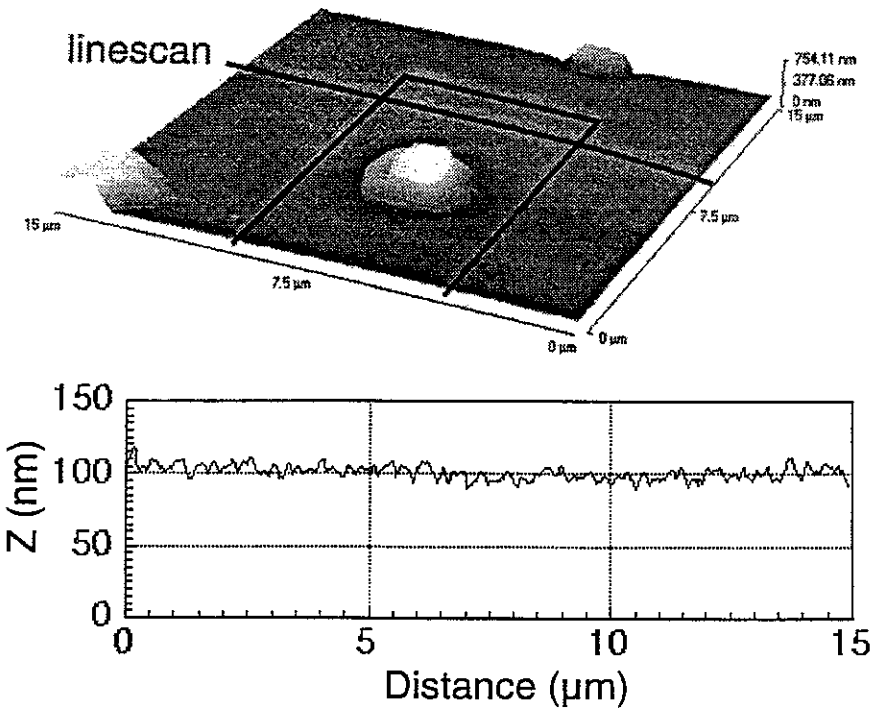

Figure 2. Atomic force micrograph of the cubic epilayer shown in figure 1. The marked area corresponds to a bright rectangle observed in the optical micrograph. The line scan across the rectangle does not show any surface structures; the measured roughness is 4 nm inside the rectangle, and 4.2 nm outside.

these being, first, bright rectangles, second, dark dots within bright rectangles and, third, dark dots outside the rectangles. The diameter of the dots is about 3 μm, and the area of the rectangles is about 10 μm $\times$ 5 μm. The rectangles are oriented along a [110] direction.

An AFM micrograph, taken at one of the rectangular structures, is shown in figure 2. While the bright rectangles of the optical micrograph do not show up in the AFM image, the dark dot is clearly seen. It can be attributed to a micrometre-size crystal which grows under a droplet of liquid Ga. Such droplets are formed by excess Ga at the surface during MBE growth. These droplets of liquid Ga are exposed to the N flux and become saturated and even oversaturated with N according to the equilibrium conditions on the surface. This induces nucleation of a single GaN crystal in the Ga melt, preferentially at screw dislocations. Further growth leads to the formation of 3D GaN microcrystals with a well-defined morphology.

AFM investigations show no difference between the surface morphology in the vicinity of the microcrystals, i.e. atop

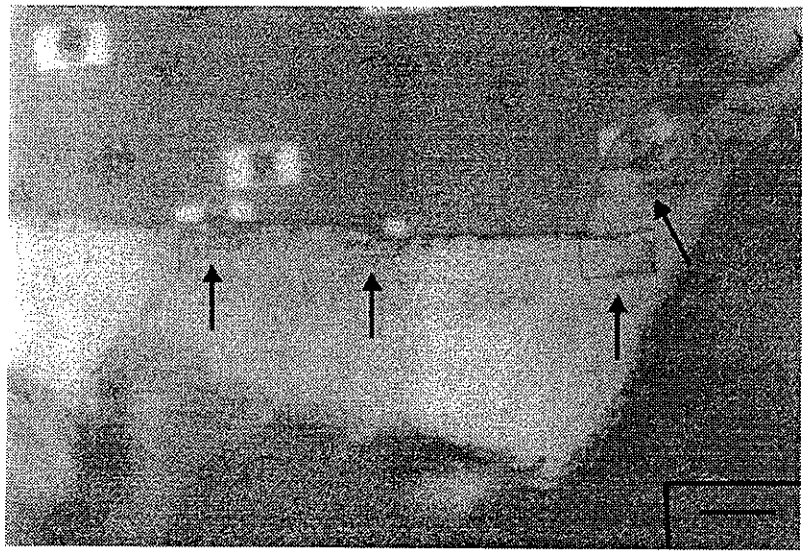

Figure 3. Optical micrograph of a region of the sample where part of the GaN epilayer was inadvertently removed during the cleavage process. The marked regions show the extension of the bright rectangles into the GaAs substrate. The scale bar in the lower right corner corresponds to 10 μm.

the rectangular structures and unperturbed areas of the epilayer. Line scans, a typical example of which is shown in figure 2, do not indicate either a variation of the film thickness possibly connected with an additional overlayer or a change in surface roughness which might account for the different reflectivity of the inclusions. Figure 3 shows an optical micrograph of a site of the sample where parts of the GaN layer were inadvertently removed from the substrate during the cleaving process. In the figure, indicated by arrows, it can be seen that the bright rectangular structures of the layer are extended into the GaAs substrate, where they show up as dark rectangular regions. This seems to indicate that the substrate is modified underneath the rectangles in the layer, yielding a different reflectivity. Indeed, in a scanning electron micrograph of the cleavage plane of this sample we find holes of micrometre extension and with a depth of about 0.2 μm in the GaAs surface region. Obviously, these holes develop after the GaN growth has started since the epilayer atop is planar. More details about the formation of these microcrystals are given in [10].

3. Micro-Raman measurements

The micro-Raman measurements were carried out at room temperature in backscattering geometry by means of a Jobin Yvon Micro Raman system, model T64000. The 5145 Å (2.41 eV) radiation of an argon ion laser was used for excitation. The beam was focused by means of a microscope of magnification 1000; the laser spot had a diameter of about 2 μm at the sample surface. The incident laser beam was polarized parallel to the (110) crystal axis, and no polarization analyser was used for the scattered beam. In order to avoid thermal damage, the laser power was kept as low as 30 mW. The Raman spectra were analysed by means of a double subtractive monochromator, having a focal length of 0.64 m and being equipped with a diffraction grating with 1800 grooves mm^{-1}. The slit width was set to 300 μm which provided us with a spectral resolution of about 5 cm^{-1}. The spectra were recorded with a CCD camera.

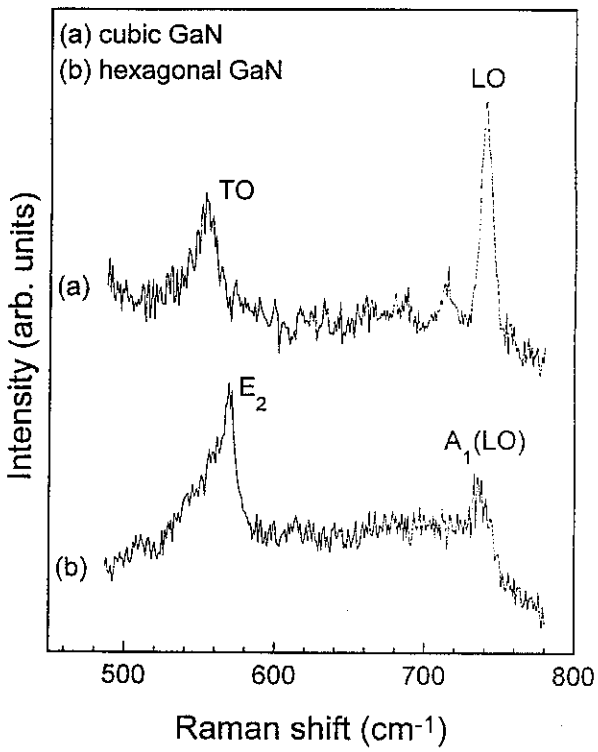

Figure 4. Conventional Raman spectra taken from a cubic and a hexagonal GaN layer in backscattering configuration. Excitation wavelength 4579 Å. $T = 300$ K.

For comparison, we also performed conventional Raman measurements on cubic and hexagonal reference layers. Typical conventional Raman spectra, taken at room temperature and in backscattering configuration, are shown in figure 4. In the cubic spectrum, the TO component of the T_2 mode shows up at 555 cm^{-1}, and the LO component of the T_2 mode is seen at 741 cm^{-1}. The TO mode is symmetry forbidden in backscattering configuration. We assumed that

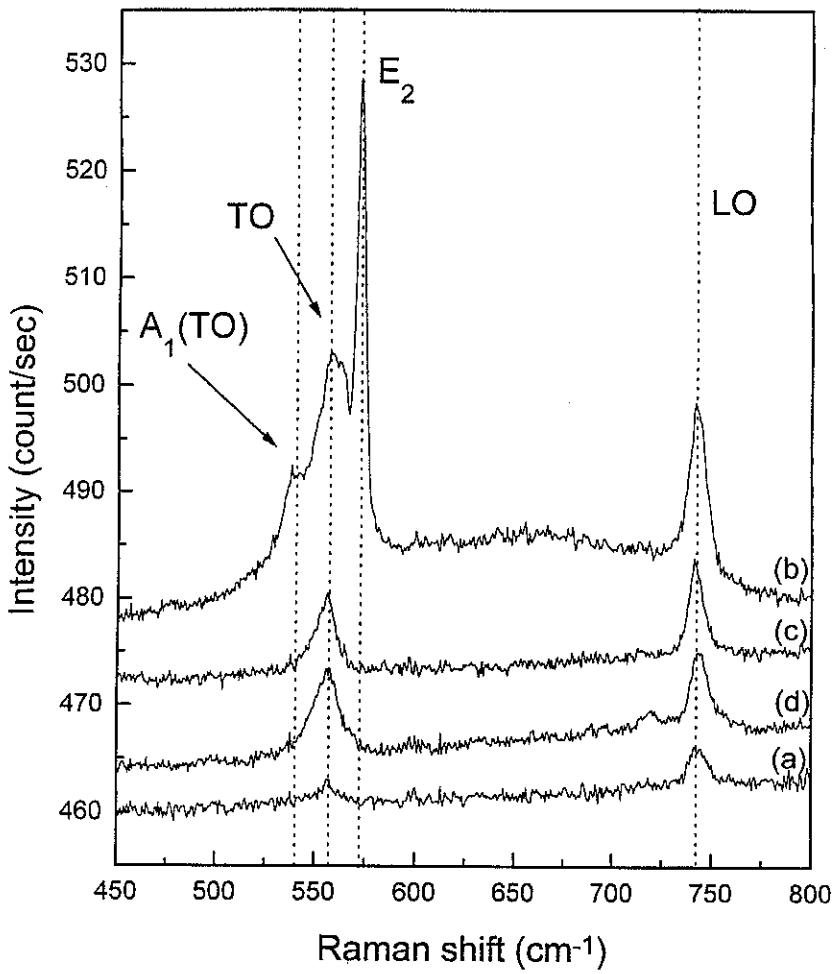

Figure 5. Micro-Raman spectra taken from different types of surface regions of our cubic GaN epilayers. The types of surface regions are identified by means of the microphotograph of figure 1 as follows: spectrum (a), areas free of inclusions; spectrum (b), inclusions seen as bright rectangles with one or more dark dots within; spectrum (c), dark dots only; spectrum (d), bright rectangles only. Excitation wavelength 5145 Å. $T = 300$ K. The spectra are shifted towards each other; however, the intensity scale is the same for all spectra shown.

short-range perturbations allow this mode [7]. It has been argued [9] that multiple reflections inside the transparent GaN layer are responsible for the observed strong TO peak. Although we of course can not rule out this possibility, one argument in favour of our interpretation is the fact that the TO component of the GaAs buffer layer in our sample is also clearly observed. In hexagonal GaN, each component of the cubic T_2 mode splits into an A_1 and an E_1 mode [7, 10–16]. In backscattering geometry, only the LO component of the A_1 mode is Raman allowed while the TO component of the A_1 mode and both the LO and the TO components of the E_1 mode are Raman forbidden. In the hexagonal spectrum of figure 4 the LO A_1 mode shows up at 733 cm^{-1}. In addition to the A_1 and E_1 modes derived from the cubic T_2 modes, two other modes occur in hexagonal GaN which do not have their counterparts in cubic GaN. Both modes, one at low frequency and one at high frequency, have E_2 symmetry and are due to the doubling of the primitive zincblende unit cell in the wurtzite structure [7, 15]. In backscattering configuration, both E_2 modes are allowed. In the hexagonal spectrum of figure 4, the high-frequency E_2 mode is seen as a strong peak at 571 cm^{-1}. The latter may be taken as an unambiguous manifestation of the hexagonal phase of GaN.

The micro-Raman spectra were taken with the incident laser beam directed at one of the following four types of surface regions: (a) areas free of irregularities, referred to as 'regular epilayer regions'; (b) dark dots within bright rectangles; (c) dark dots within regular epilayer regions; (d) bright rectangles only. Comparing the diameter of the laser beam (2 μm) with the lateral extensions of the irregularities (b), (c) and (d), we conclude that at least 90% of the recorded spectra should be due to the irregularity type the laser is focused at. The lateral distances between different inclusions are typically larger than 10 μm. Thus, Raman spectra taken with the laser focused at half-distance between two irregularities should be 100% due to a region of type (a). In fact, we find that Raman spectra taken from regions of the same type are identical, or almost identical, while spectra from regions of different types are different. Figure 5 shows typical Raman spectra of the four region types.

Spectrum (a), recorded from a regular epilayer region, shows two peaks at 555 cm^{-1} and 741 cm^{-1} which are clearly due to the cubic TO and LO modes of GaN, respectively.

Spectrum (b), taken from a dark dot within a bright rectangle, is dominated by the strong peak at 571 cm^{-1}, this being the position of the E_2 mode of hexagonal GaN. This finding indicates that the region in the sample corresponding to the hexagonal structure is free from large strain. The peak at 555 cm^{-1} corresponds to the cubic TO mode. Slightly above the cubic TO peak, at 560 cm^{-1}, the TO component of the hexagonal E_1 mode shows up, and slightly below this peak, at 540 cm^{-1}, one has the TO component of the hexagonal A_1 mode. This phonon occurs in the range 531–537 cm^{-1} [7]. Taking into consideration the spectral resolution in our experiments the assignment of this phonon seems to be correct. Since the TO phonon energy of the cubic phase is clearly identified in the spectrum we expect to detect also the LO phonon. Indeed, a relatively strong hight-frequency peak located at 741 cm^{-1} occurs in the spectrum which can then be ascribed to the LO phonon of cubic GaN. However, we are not in a position to exclude in our experiment the possibility of this peak also having a contribution of the E_1 (LO) mode of hexagonal GaN which occurs in the range 741–745 cm^{-1} [7].

Spectra (c) and (d) of figure 5, stemming, respectively, from a dark dot outside a bright rectangle and from a bright rectangle itself, exhibit only the two cubic TO and LO peaks of GaN.

The micro-Raman spectra allow us to identify the structures of the four surface regions investigated. We conclude that the dark dots are associated with GaN microcrystals of either wurtzite structure—this applies for dots surrounded by bright rectangles—or zincblende structure—this is valid for dots not surrounded by rectangles.

The bright rectangles around the microcrystals are regions of cubic GaN, just as the regular GaN epilayer. The optical contrast between the rectangles and the regular epilayer seems to be due to micrometer-size rectangular holes at the GaAs surface. There is experimental evidence that the formation of such holes proceeds by remelting of parts of the GaN–GaAs interface region [10]. In a first step, the unsaturated Ga droplets etch back the thin GaN overlayer which has been grown during the nucleation stage. If the Ga melt reaches the GaAs surface, a certain amount of GaAs is remelted because of the high solubility of As in liquid Ga at 700 °C, resulting in rectangular etch holes. If the Ga droplets are saturated with As and N, the remelting process stops and GaN microcrystals start to grow within the Ga droplets. Because of the dissolution of the cubic GaN film under the droplets, the nucleation of these microcrystals is not influenced by the cubic epitaxial layer and, therefore, the more stable hexagonal structure dominates. This explains the existence of hexagonal microcrystals under Ga droplets which are involved in the remelting process. The growth of other microcrystals, not connected with the remelting process, follows the orientation of the cubic GaN layer. The optical contrast between the rectangles and the regular epilayers is due to the reflectivity difference between the frozen, polycrystalline GaAs–Ga solution in the rectangular holes and the surrounding monocrystalline GaAs.

4. Conclusions

Commonly, in MBE growth of cubic GaN on a (001) GaAs substrate, a slight Ga excess is used in order to avoid larger hexagonal inclusions. If the Ga excess is too large, it results in the formation of Ga droplets on the epilayer surface. Micro-Raman spectroscopy reveals that, below these droplets, GaN microcrystals of either cubic or hexagonal phases exist. Around the hexagonal microcrystals, cubic GaN regions are formed which are seen as bright rectangles in optical micrographs. These rectangles seem to be due to the formation of small regions of a free-standing GaN film on top of small holes in the substrate which are formed during the epilayer growth.

Acknowledgments

The authors would like to thank CNPq, CAPES, FINEP and FAPESP (grant 97/11959-2), Brazilian founding agencies, the German Science Foundation (DFG) and DAAD for partial financial support.

References

[1] Morkoç H, Strite S, Gao G C, Lin M E, Sverdlov B and Burns M 1994 *J. Appl. Phys.* **76** 1363–98
[2] Schikora D, Hankeln M, As D J, Lischka K, Waag A, Buhrow T and Henneberger F 1996 *Phys. Rev.* B **54** R8381–4
[3] Brandt O, Yang H, Jenichen B, Suzuki Y, Däweritz L and Ploog K 1995 *Phys. Rev.* B **52** R2253–6
[4] Cheng T S, Jenkins L C, Hooper S E, Foxon C T, Orton J W and Lacklison L E 1996 *Appl. Phys. Lett.* **66** 1509–11
[5] As D J, Schikora D, Greiner A, Lübbers M, Mimkes J and Lischka K 1996 *Phys. Rev.* B **54** R11 118–21
[6] As D J, Schmilgus F, Wang C, Schöttker B, Schikora D and Lischka K 1997 *Appl. Phys. Lett.* **70** 1311–13
[7] Tabata A, Enderlein R, Leite J R, da Silva S W, Galzerani J, Schikora D, Kloidt M and Lischka K 1996 *J. Appl. Phys.* **79** 4137–9
[8] Siegle H, Eckey L, Hoffmann A, Thomson C, Meyer B K, Schikora D, Hankeln M and Lischka K 1995 *Solid State Commun.* **96** 943–9
[9] Giehler M, Ramsteiner M, Brandt O, Yang H and Ploog K 1995 *Appl. Phys. Lett.* **67** 733–5
[10] Lima A P, Frey T, Köhler U, Wang C, As D J, Schöttker B, Lischka K and Schikora D 1999 *J. Crystal Growth* **197** 31–6
[11] Manchon D D Jr, Barker A S, Dean P J Jr and Zetterstrom R B 1970 *Solid State Commun.* **8** 1227–31
[12] Lemos V, Argüello C A and Leite R C C 1972 *Solid State Commun.* **11** 1351–3
[13] Burns G, Dacol F, Marinace J C and Scott B A 1973 *Appl. Phys. Lett.* **22** 356–7
[14] Cingolani A, Ferrara M, Lugara M and Scamarcio G 1986 *Solid State Commun.* **58** 823–4
[15] Nakahara J, Kuroda T, Amano H, Akasaki I, Minomura S and Grzegory I 1990 *9th Symp. on Record of Alloy Semiconductor Physics and Electronics (Izunagaoka, 1990)* p 391
[16] Perlin P, Jauberthie-Carillon C, San Miguel J P I A, Grzegory I and Polian A 1992 *Phys. Rev.* B **45** 83–9
[17] Kozawa T, Kachi T, Kano H, Taga Y and Hashimoto M 1994 *J. Appl. Phys.* **75** 1098–101